

## Location of the Fracture Faces Within the Cell Envelope of *Acinetobacter* Species Strain MJT/F5/5

U. B. SLEYTR,<sup>1</sup> MARGARET J. THORNLEY,<sup>2</sup> AND AUDREY M. GLAUERT

*Strangeways Research Laboratory, Cambridge, England*

Received for publication 20 November 1973

The cell wall of the gram-negative bacterium *Acinetobacter* species strain MJT/F5/5 shows in thin section an external "additional" layer, an outer membrane, an intermediate layer, and a dense layer. Negatively stained preparations showed that the additional layer is composed of hexagonally arranged subunits. In glycerol-treated preparations, freeze-etching revealed that the cell walls consist of four layers, with the main plane of fracture between layers cw 2 and cw 3. The surface of cw 2 consisted of densely packed particles, whereas cw 3 appeared to be fibrillar. In cell envelopes treated with lysozyme by various methods, the removal of the dense layer has detached the outer membrane and additional layer from the underlying layers, as shown in thin sections. When freeze-etched in the absence of glycerol, these detached outer membranes with additional layers fractured to reveal both the faces cw 2 and cw 3 with their characteristic surface structures, and, in addition, both the external and internal etched surfaces were revealed. This experiment provided conclusive evidence that the main fracture plane in the cell wall lies within the interior of the outer membrane. This and other evidence showed that the corresponding layers in thin sections and freeze-etched preparations are: the additional layer, cw 1; the outer membrane, cw (2 + 3); and the intermediate and dense layers together form cw 4. Because of similarities in structure between this *Acinetobacter* and other gram-negative bacteria, it seemed probable that the interior of the outer membrane is the plane most liable to fracture in the cell walls of most gram-negative bacteria.

The structure of the cell envelopes of gram-negative bacteria, as revealed by freeze-etching, is still the subject of some uncertainty in interpretation, because it is difficult to correlate the results of freeze-etching with those obtained from observations on thin sections and negatively stained preparations. In particular, the location of fracture planes within the cell wall, in relation to structures seen in section, is not well established (10). In an earlier study (15) of another *Acinetobacter* strain, MJT/F5/199A, we suggested that fracture might take place between the outer membrane and the intermediate layer, but the evidence did not exclude the possibility of internal fracture of the outer membrane. To resolve this point, we have studied a different strain of *Acinetobacter*, MJT/F5/5, which like strain 199A has a surface

composed of regularly arranged subunits which provide a useful marker for the outer surface of the outer membrane. In strain 5, however, various methods of separation of the layers of the cell wall gave useful results. One particular method of lysozyme treatment resulted in spherical ghosts which could be freeze-etched in the absence of sucrose or glycerol to reveal two internal fracture faces and both the external and internal etched faces of the outer membrane, thus proving that internal fracture of the outer membrane does take place.

The classification of MJT/F5/5 strain in the genus *Acinetobacter* is well established, because in the taxonomic survey of Thornley (18) it was included in the oxidase-negative Phenon 4iii, and in the transformation system of Juni (7) it showed the transformation reaction considered to be typical of *Acinetobacter*.

It was also of interest to compare results for strain MJT/F5/5 with those obtained for the oxidase-positive *Acinetobacter* strain MJT/F5/199A, which has tetragonally arranged

<sup>1</sup> Present address: Institute of Food Technology, University of Agriculture, A-1180 Vienna, Austria.

<sup>2</sup> Present address: Dept. of Pathology, University of Cambridge, Addenbrooke's Hospital, Hills Road, Cambridge, England.

subunits on the cell surface and which has already been extensively studied by electron microscopy and chemical methods (15, 17, 19, 20; M. J. Thornley et al., *Phil. Trans. Roy. Soc. London*, in press).

### MATERIALS AND METHODS

*Acinetobacter* sp. strain MJT/F5/5, from M.J.T.'s culture collection, was grown in a FE 007 fermenter (Biotec Ltd., Selsdon, South Croydon CR2 87D, England) by using maximum aeration at a temperature of 28 to 30 C. The fermenter contained 700 ml of heart infusion broth (Difco) with 0.01% CaCl<sub>2</sub> and 0.1 ml of silicone MS Antifoam A (Hopkin & Williams Ltd., Chadwell Heath, Essex, England). Cultures were harvested in the mid-logarithmic phase. For comparison, other cultures were grown in the same medium in conical flasks, aerated by shaking at 28 C, and harvested in the late logarithmic phase. No differences were observed between cells grown by the two methods, so no distinction will be made between growth conditions in the later descriptions of methods.

Cells to be freeze-etched were centrifuged from the growth medium, and the pellet was examined without washing, because it was found that washing twice with 0.85% NaCl did not result in a clearer picture of the etched outer surfaces of the cells. For freeze-etching in the presence of glycerol, 25% vol/vol of glycerol was added to suspensions of cells in the growth medium; they were then left at 24 C for 1 h before centrifugation and freeze-etching of the pellet.

The effects of a mild heat treatment were studied. Cells from a portion of the culture were washed in 0.05 M phosphate buffer, pH 7.4, and suspended in the same buffer. A tube containing this suspension was placed in a water bath at 60 C for 25 min, during which time the temperature of the suspension was between 55 and 60 C for 20 min. After this, the suspension was cooled, glycerol at 30% vol/vol was added, and, after 30 min at 24 C, the suspension was centrifuged, and portions of the pellet were examined by freeze-etching and negative staining and fixed for thin-sectioning.

Various methods of treatment with lysozyme were applied, because it was intended to freeze-etch spheroplasts in the presence of sucrose and glycerol and also to examine cell envelopes by deep-etching without glycerol. Method A was to wash the cells in 0.05 M phosphate buffer, pH 7.4, and to suspend them in the same buffer containing 10% wt/vol sucrose and 30% vol/vol glycerol. After 1 h at 25 C, 1.25 mM ethylenediaminetetraacetate (disodium salt) and 100 µg of lysozyme per ml were added. The mixture was incubated at 25 C for 30 min and centrifuged; the pellet was examined by freeze-etching and phase-contrast microscopy, which showed that most cells retained their rod shape and their contents; only a few had become spherical.

Method B was to incubate a suspension similar to that used in method A for 1 h at 25 C, after the addition of lysozyme, and then to keep this suspension at 5 C for 17 h, followed by centrifugation and

examination. About one-half of the cells had become spherical, whereas others were normal or swollen rods.

Method C consisted of washing and resuspending cells in 0.05 M phosphate buffer, pH 7.4, adding 100 µg of lysozyme per ml and 1.25 mM ethylenediaminetetraacetate to the suspension and incubating with stirring at 25 C for 5 min. After this, 20 mM MgCl<sub>2</sub> was added, and incubation was continued for 30 min. The suspension was then centrifuged, and the pellet was suspended in phosphate buffer, to which 30% vol/vol of glycerol was added. This suspension was left at 25 C for 1 h, then centrifuged, and the pellet was examined by freeze-etching. The cells remained rod-shaped during the incubation with lysozyme, but changed to swollen forms in the presence of glycerol.

In method D, cells were washed with 0.05 M tris(hydroxymethyl)aminomethane-hydrochloride buffer, pH 8.0, and suspended in the same buffer, to which lysozyme at 100 µg/ml and then ethylenediaminetetraacetate at 1.25 mM were added. After 1 min at 25 C, 20 mM MgCl<sub>2</sub> was added, and, after a further period of 1 min, the suspension was centrifuged. The pellet consisted mainly of spherical cells which had lost much or all of their contents; some distorted rods were also present.

Method E consisted of breakage of the cells in the Mickle disintegrator followed by lysozyme treatment of the cell envelopes. Cells were washed in 0.05 M phosphate buffer, pH 7.4, and suspended in 0.2 M NaCl solution. A portion (10 ml) of this suspension with 10 g of Ballotini beads grade 12 was treated in the Mickle disintegrator for 1 min. Fragments of the cell envelopes adhered to the glass beads, and were removed by washing the beads on a sintered filter with M NaCl. The fragments were centrifuged from the M NaCl solution, the pellet was suspended in 0.05 M phosphate buffer, pH 7.4, containing 20 mM MgCl<sub>2</sub>, and 100 µg of lysozyme per ml was added. The suspension was stirred for 25 min at 25 C and then centrifuged. The pellet was examined by freeze-etching and negative staining, and thin sections were prepared.

Freeze-etching was carried out in a Balzer's freeze-etch apparatus (model BA 360 M) as described by Moor and Mühlethaler (8). The replicas were cleaned in 30% chromic acid, rinsed in distilled water, and mounted on Formvar-coated grids.

For thin sections, preparations were fixed in 2.5% glutaraldehyde in 0.09 M cacodylate buffer, pH 7.2, containing 3 mM CaCl<sub>2</sub> for 1 h at 20 C, and washed overnight at 4 C in the cacodylate buffer. The preparations were post-fixed with Zetterqvist's Veronal-acetate-buffered osmium tetroxide, pH 7.2, for 1 h at 20 C, stained with 0.5% uranyl acetate in Veronal-acetate buffer for 1 h, dehydrated in ethanol, and embedded in Araldite. Thin sections were cut with glass knives on a LKB Ultratome III or a Cambridge-Huxley ultramicrotome and stained with lead citrate.

For negative staining, 1% ammonium molybdate, pH 7.0, was used.

Specimens were examined in an AEI EM 6B electron microscope operating at 60 kV with a 50-µm objective aperture.

## RESULTS

The appearance of the cell wall of *Acinetobacter* strain MJT/F5/5 in thin section, already known from earlier work (6), is indicated diagrammatically in Fig. 1A and illustrated in Fig. 15. Outside the plasma membrane, the dense layer, intermediate layer, and outer membrane are arranged as is typical for gram-negative bacteria, and an additional layer, with a less distinct outline, is believed to correspond to an external layer of hexagonally arranged subunits (6). Diagrams showing our interpretation of the layers revealed by the freeze-etching technique in cross-fractured cell walls (Fig. 1B) and after an oblique fracture, seen from the convex side (Fig. 1C), are placed adjacent to the diagram of the cell wall, as seen in thin section (Fig. 1A), so that the structures which we believe to correspond may be compared. The appearance of the layers revealed by an oblique fracture, seen from the concave side, is also indicated (Fig. 1D). The reasons for the interpretations shown in Fig. 1 are explained as the relevant results are described.

The bacterium examined (*Acinetobacter* strain MJT/F5/5) is a nonmotile short rod, and, when intact cells are freeze-etched in the absence of glycerol, the outer surface, revealed by etching, consists of a hexagonal array of subunits with a center-to-center spacing of approximately 11 nm (Fig. 2, 3). After growth under the different conditions tested, the surface appearance was similar, with adjacent small areas having a different orientation of the regular pattern and being joined by slightly irregular regions analogous to the "grain boundaries" between crystallites. Even larger areas where the direction of the pattern appears to be uniform show many "faults" in the structure (Fig. 3). In a few cells, areas lacking subunits were observed (Fig. 3, arrows); these areas could not have been exposed by fracture, because some of them are not at the highest part of the exposed portion of the cell.

The appearance of this hexagonal array after negative staining can only be seen on specially treated cells or on fragments of cell wall. A few cells in the heat-treated preparations (Fig. 4) show folds, presumed to consist of the outer layers of the cell envelope, extending around the dense mass representing the cell contents. The folded edge appears as a light line, separated by a darker region from the rest of the cell, which is seen in surface view to be covered with extensive patterned regions. Broken fragments of cell wall, treated with lysozyme (method D) to remove the peptidoglycan and leave the outer

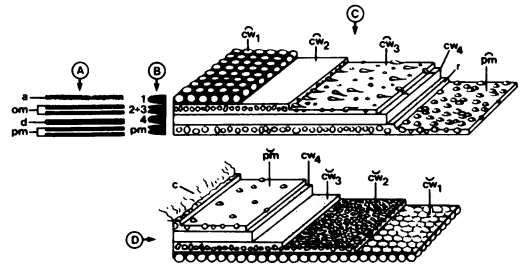


FIG. 1. Diagram showing the relationship between the layers of the cell envelope revealed in thin section and in preparations freeze-etched in the presence of glycerol. (A) Cell envelope as seen in thin section. The innermost layer is the plasma membrane (pm), which is surrounded by the layers of the cell wall: the dense layer (d), the intermediate layer, the outer membrane (om), and the additional layer (a). (B) Cell envelope as it appears after cross fracture in a freeze-etched preparation. The four main ridges represent the plasma membrane (pm) and the layers of the cell wall: cw 4, cw (2 + 3), and cw 1. Both the plasma membrane and cw (2 + 3) appear as double ridges in many preparations. It is concluded (see text) that cw 4 corresponds to the dense and intermediate layers as seen in section, cw (2 + 3) represents the outer membrane, and cw 1 represents the additional layer. (C) An obliquely fractured cell envelope seen from the convex side in a freeze-etched preparation. The etched outer surface (cw 1) consists of hexagonally arranged subunits and lies next to the fracture face  $c\hat{w}$  2, of which small areas are seen occasionally. The main convex fracture face in the cell wall,  $c\hat{w}$  3, appears fibrillar, and is separated by ridges representing the edges of cw 4 and the outer portion of the plasma membrane (r) from the internal fracture face of the plasma membrane ( $p\hat{m}$ ). (D) Obliquely fractured cell envelopes seen from the concave side show the cytoplasm (c), the concave internal fracture face of the plasma membrane ( $p\hat{m}$ ), a ridge representing the edge of cw 4, and  $c\hat{w}$  3, which is only seen as a fracture face in exceptional preparations (see Fig. 8) but which is revealed by etching in lysozyme-treated preparations without glycerol. When  $c\hat{w}$  3 is not revealed, the edges of cw 4 and cw 3 are often united in one ridge. The main concave fracture face in the cell wall,  $c\hat{w}$  2, has a granular surface; the adjacent face,  $c\hat{w}$  1, is revealed occasionally in small areas, which are usually smooth but which sometimes show traces of the hexagonal pattern.

membrane, become folded into tubules and vesicles (Fig. 5), but a few areas show a single layer of the hexagonal array. By this technique, the array appears as a pattern of small white dots separated by dark areas. Some indication of individual subunits may be seen at the folded edges of these small fragments (Fig. 5, arrows).

In cells freeze-etched in the absence of glycerol, the edges of only two layers could be seen in the fractured cell walls (Fig. 2), and only very

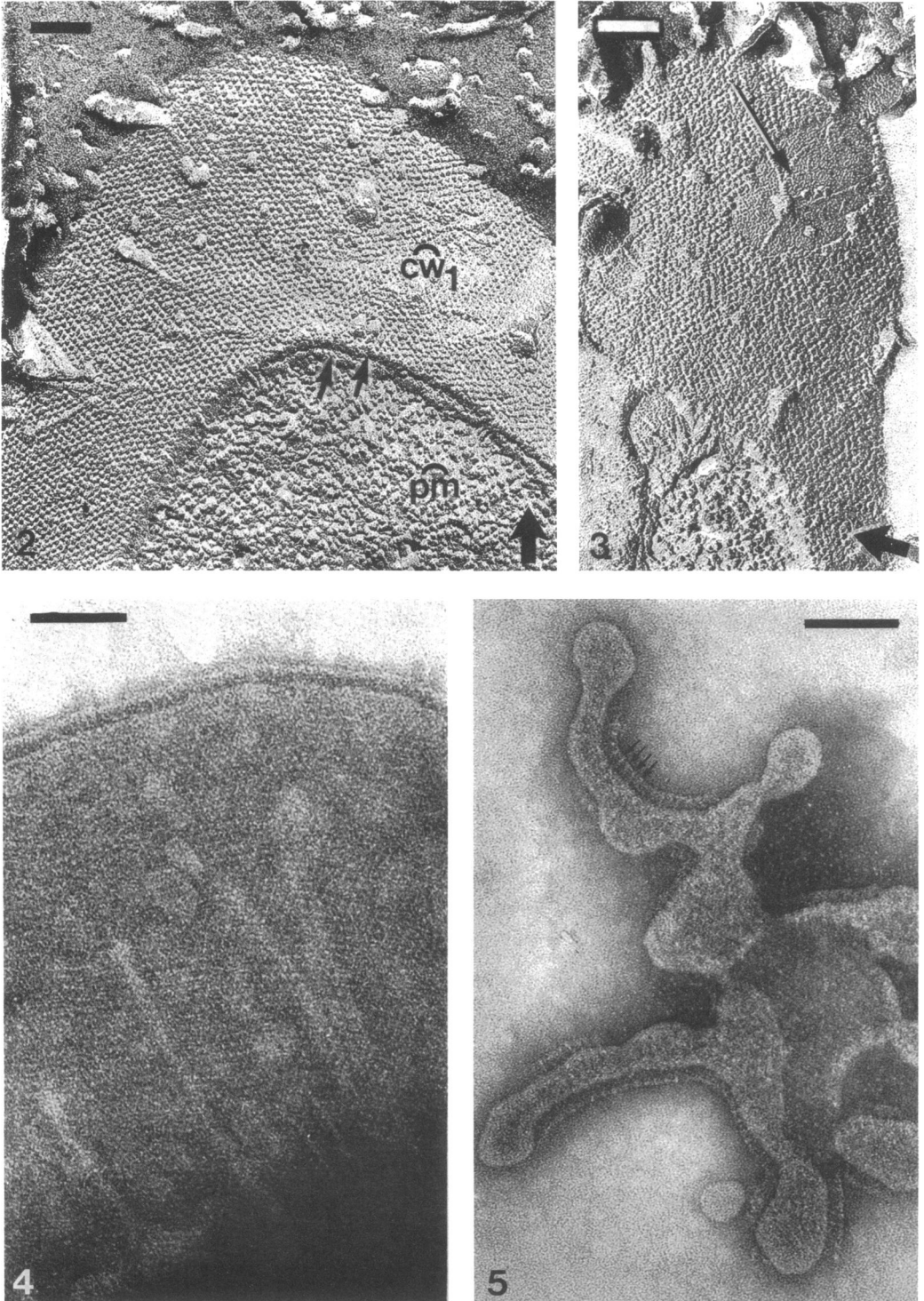


FIG. 2-30. Electron micrographs of preparations of *Acinetobacter* sp. strain MJT/F5/5. In freeze-etched preparations, the direction of shadowing is indicated by an arrow in the lower righthand corner. Abbreviations are as listed in Fig. 1. The magnification markers in all figures represent 0.1  $\mu\text{m}$ .

FIG. 2. A cell freeze-etched in the absence of glycerol. The outer surface ( $\widehat{cw}1$ ) revealed by etching consists of hexagonally arranged subunits. The fractured edges of the cell wall show two ridges (arrows);  $\widehat{pm}$ , internal fracture face of the plasma membrane.

FIG. 3. An area lacking subunits (arrow) forms part of the outer surface of this cell, freeze-etched in the absence of glycerol.

small areas of the characteristic fracture faces were exposed. Treatment of the preparations with 25 or 30% vol/vol glycerol before freeze fracture induced several changes. The layers appeared more widely separated in cross fracture, the number of edges apparent in oblique fracture was four, and the areas of the main fracture faces within the cell wall were much increased, whereas the area of the internal fracture of the plasma membrane was unaffected. Figure 6 shows the convex view of a cell after an oblique fracture in the presence of glycerol, as shown diagrammatically in Fig. 1C. A small area of the outer surface with the regular array of subunits (cw 1) is exposed, and within this lies the fractured edge of cw 2. In a very few fractured cells, a small area of the smooth convex surface of cw 2 is seen (Fig. 7). The main fracture plane in the cell wall lies between cw 2 and cw 3, and the convex face, cw 3 (Fig. 6, 7), is covered by a large number of fibrils, some of which extend over its surface from the broken edges of the outer layers cw 1 and 2, and some of which originate from the surface of cw 3 itself. Most of these fibrils show a radial arrangement, pointing inwards from the broken edges of the outer layers. A few granules and depressions are visible also on this fracture face. Where inner layers of the cell envelope are exposed (Fig. 6), the edge of cw 3 is seen to lie next to ridges representing cw 4 and the outer portion of the plasma membrane. The internal fracture face of the plasma membrane, with numerous irregularly arranged particles, is exposed.

In concave view, cell envelopes obliquely fractured in the presence of glycerol (Fig. 1D, 8, 9, 11) show the edge of cw 1, and occasionally small areas of its inner surface (cw 1) are revealed; in Fig. 11, this surface shows a hexagonal pattern similar to that on the outside of the cell, although less well marked, and must therefore represent the inner surface of the layer containing the hexagonally arranged subunits.

The main fracture plane in the wall, seen from the concave side, forms the surface of cw 2, which consists of densely packed irregularly arranged particles smaller than those seen on the fracture faces of the plasma membrane (Fig. 8, 9, 11). The layers cw 3 and cw 4 often show only one fractured edge in concave view (Fig. 9,

11), but in the cell envelope shown in Fig. 8 the inner part of the envelope has been folded upwards by the fracture, exposing a smooth surface, which is thought to be cw 3, whereas the thick folded region consists of cw 4 and the outer portion of the plasma membrane. The exposed concave fracture face of the plasma membrane has the appearance usually found in bacteria, with particles less densely packed than those of the convex fracture face of the plasma membrane.

The appearance of envelopes of both normal and heat-treated cells after cross fracture in the presence of glycerol may be compared with their appearance in thin section in Fig. 10, 12-15. The interpretation of the structures seen is indicated in Fig. 1A and B. The cross-fractured envelopes of normal cells show four layers of approximately equal thickness, including the plasma membrane (Fig. 13, 16); these layers are even more clearly distinguished after mild heat treatment which causes greater separation between the layers (Fig. 10). This more distinct separation between the layers is also seen in thin sections of heat-treated cells (Fig. 14) compared with normal cells (Fig. 15). After freeze-etching, a double ridge is visible at the cross-fractured edges of two of the layers, the plasma membrane and the central layer of the three structures forming the cell wall (Fig. 10, 13). Therefore, it seems that the layers showing double ridges in cross fracture correspond to those which appear as "unit membranes" in thin section (Fig. 1A and B). These diagrams show that the additional layer seen in section is represented by cw 1 in freeze-etched preparations, the outer membrane corresponds to cw (2 + 3), and the intermediate and dense layers correspond to cw 4. The notation cw (2 + 3) is adopted for the second layer, because experiments described later show that the fracture between cw 2 and cw 3 is an internal fracture of the outer membrane.

The suggestion that the cross-fractured layer cw (2 + 3) represents the outer membrane, as seen in thin section, is reinforced by observations on the arrangement of the layers during cell division and bleb formation. This bacterium divides by a process of constriction combined with the ingrowth of a septum, and the participation of the different layers of the enve-

FIG. 4. *Negatively stained preparation showing the edge of a heat-treated cell. The cytoplasm is confined to a densely stained central zone, surrounded by flatter folded portions of the cell envelope, which show extensive areas of the regular pattern.*

FIG. 5. *Negatively stained preparation of a fragment of the cell wall, treated with lysozyme by method E. The outer membrane and additional layer remain (see Fig. 30), and at the edges of the fragment form small tubules, where some indication of the individual subunits may be seen in side view (arrows). Hexagonal pattern is visible on a central portion of the fragment.*

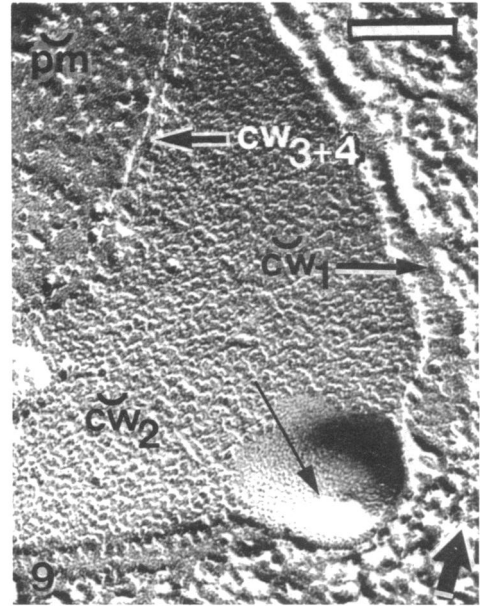
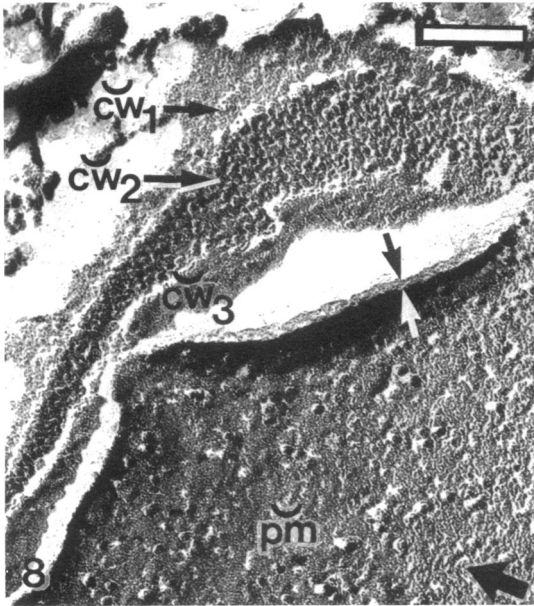
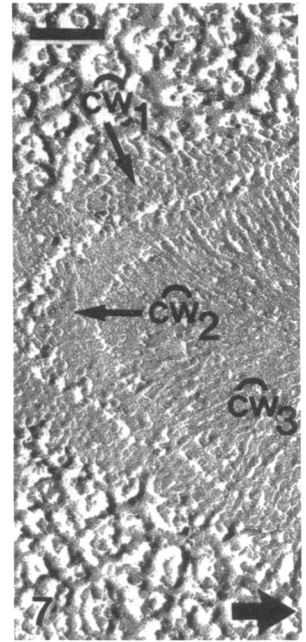
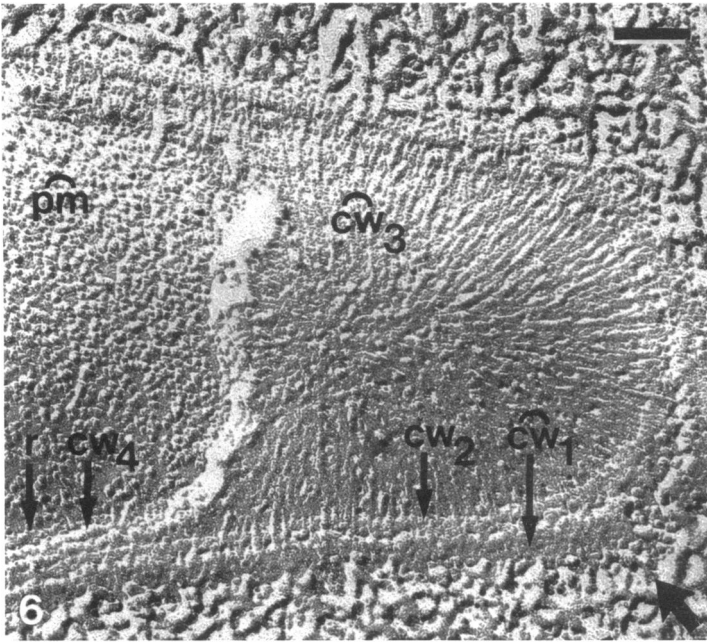


FIG. 6-9. Preparations freeze-etched in the presence of glycerol.

FIG. 6. Convex view of an obliquely fractured cell envelope (see Fig. 1C). A small area of the outer surface  $c\tilde{w}$  1 has been exposed by etching and shows the regular array of subunits. The edge of  $cw$  2 adjoins the main convex fracture face in the cell wall,  $c\tilde{w}$  3, whose surface shows radially arranged fibrils and a few granules and depressions. The edges of  $cw$  4 and the outer portion of the plasma membrane ( $r$ ) lie next to the internal fracture face of the plasma membrane ( $pm$ ).

FIG. 7. Portion of the convex side of an obliquely fractured cell envelope which shows a small area of  $c\tilde{w}$  2. Outer surface of the cell,  $c\tilde{w}$  1, shows the regular array of subunits.

FIG. 8. Concave view of an obliquely fractured cell envelope (see Fig. 1D). A small area of  $c\tilde{w}$  1 adjoins the granular surface of  $c\tilde{w}$  2, the main concave fracture face in the cell wall. A portion of the inner layers of the envelope has been folded upwards by the fracture, exposing a smooth surface ( $c\tilde{w}$  3) not normally seen. Thick folded edge (arrows) is thought to consist of  $cw$  4 and the outer portion of the plasma membrane;  $pm$ , the concave internal fracture face of the plasma membrane.

FIG. 9. Another concave view of an obliquely fractured cell envelope, which shows the same layers as in Fig. 8, except that  $c\tilde{w}$  3 is not revealed, and the edges of  $cw$  4 and  $cw$  3 appear together as an irregular ridge. This appearance is much more common than that seen in Fig. 8. The fracture face  $c\tilde{w}$  2 consists of closely packed granules, but where it continues into a protruding bleb, its surface is smooth (arrow).

lope in this process is shown (Fig. 12, 13). In thin section (Fig. 12), the additional layer and outer membrane form the boundary of the constricted zone, whereas the septum extends right across the dividing cell and is continuous with the dense layer of the cell wall. After freeze-etching in the presence of glycerol (Fig. 13), cw 1 and cw (2 + 3) show slight constriction only, whereas cw 4 is continuous with the ingrowing septum. A double ridge is formed by cw (2 + 3) in Fig. 13, as in Fig. 10.

Normal cells freeze-etched in the presence of glycerol showed some blebs in the surface, and the layers of the envelope involved in bleb formation can be inferred from Fig. 9 and 16. Figure 9 shows that the concave fracture face  $\hat{c}w$  2 continues into the bleb, but that the characteristic granular appearance of this face changes to a smooth surface within the bleb. In Fig. 16, a bleb is revealed as a convex fracture face bounded by a fractured edge. At the base of the bleb, both these layers are continuous with cw (2 + 3). It seems clear, therefore, that layer cw (2 + 3), but not cw 4, is involved in bleb formation and that fractures between cw 2 and cw 3 can extend through the blebs, exposing fracture faces which differ in surface view from those which occur in the main part of the envelope, because they lack the granular or fibrillar appearance of  $\hat{c}w$  2 or  $\hat{c}w$  3. In Fig. 16, layer cw 1 is clearly not involved in bleb formation, but it is not known whether this is always the case.

The remainder of this paper concerns experiments which were designed to shed some light on the nature and location of the main fracture plane in the cell wall, between cw 2 and cw 3. It has been observed in numerous membrane systems that glutaraldehyde fixation does not alter the characteristics of the fracture faces and the predisposition to fracture along the interior of the membrane (1). In our experiments, cells of *Acinetobacter* MJT/F5/5, previously treated with glycerol for 1 h and then fixed with glutaraldehyde, were freeze-etched. Although the internal fracture faces of the plasma membrane were revealed as usual, fracture within the cell wall was completely prevented. Cross-fractured cell envelopes showed the usual pattern of four ridges.

Heat-treated intact cells, as already mentioned, showed more distinct separation of the layers of the cell envelope (Fig. 10, 14), and when such cells were freeze-etched in the presence of glycerol large areas of the fracture faces  $\hat{c}w$  2 and  $\hat{c}w$  3 were revealed, much greater than those shown after glycerol treatment only. The

characteristic granular and fibrillar surfaces of the two fracture faces were the same as in normal glycerol-treated cells.

Treatment of intact cells with lysozyme by method A, followed by freeze-etching in the presence of glycerol, allows the cells to retain their cytoplasm, while some remain rod-shaped and others become more or less spherical (Fig. 17-19). Layers cw 1 and cw (2 + 3) become detached from the inner layers of the envelope, and cw 4 is no longer visible. Vesicles, possibly originating from everted mesosomes, are present between the remaining layers of the cell wall and the plasma membrane. In cross fracture, layer cw (2 + 3) shows a double ridge (Fig. 17, 19), and both the characteristic fracture faces are associated with layer cw (2 + 3). Figure 18 shows the concave face  $\hat{c}w$  2 with closely packed granules. In Fig. 19, a cross-fractured portion of the envelope is continuous with a region of more oblique fracture where the fibrillar fracture face  $\hat{c}w$  3 is exposed. The double ridge cw (2 + 3) seen in cross fracture (Fig. 19, double arrow) separates to reveal an internal fracture face (cw 3) which must lie between the layers represented by the two ridges. The appearance of  $\hat{c}w$  3 adjacent to the ridge of cw 2 may be compared with that of the inner face of the plasma membrane (pm) lying next to the ridge (r) representing the edge of the outer portion of the plasma membrane.

To compare these fracture faces with the etched surfaces of the same structure, it was necessary to freeze-etch lysozyme-treated cell envelopes without sucrose or glycerol. These envelopes were prepared by method D, which included stabilization by the addition of  $MgCl_2$  instead of sucrose, and during this process the cells became spherical and lost a large part of their cytoplasm. Thin sections show that the dense layer has been removed from the envelope, leaving the outer membrane and plasma membrane separated by a light space; in places, the protoplast has retracted some distance from the outer membrane (Fig. 29). After freeze-etching, the convex views of two cell envelopes are shown in Fig. 20 and 22. In Fig. 22, the fracture reveals  $\hat{c}w$  3, with its usual fibrillar appearance, surrounded by a small etched area of  $\hat{c}w$  1 with its surface subunits. In Fig. 20, the fracture has broken the surface of  $\hat{c}w$  3, and a depression has been produced by etching of the underlying material. From the appearance in section (Fig. 29), it is evident that the ice-filled region corresponds with the space between the outer membrane and the plasma membrane, and therefore the etched face of  $\hat{c}w$  1 and the

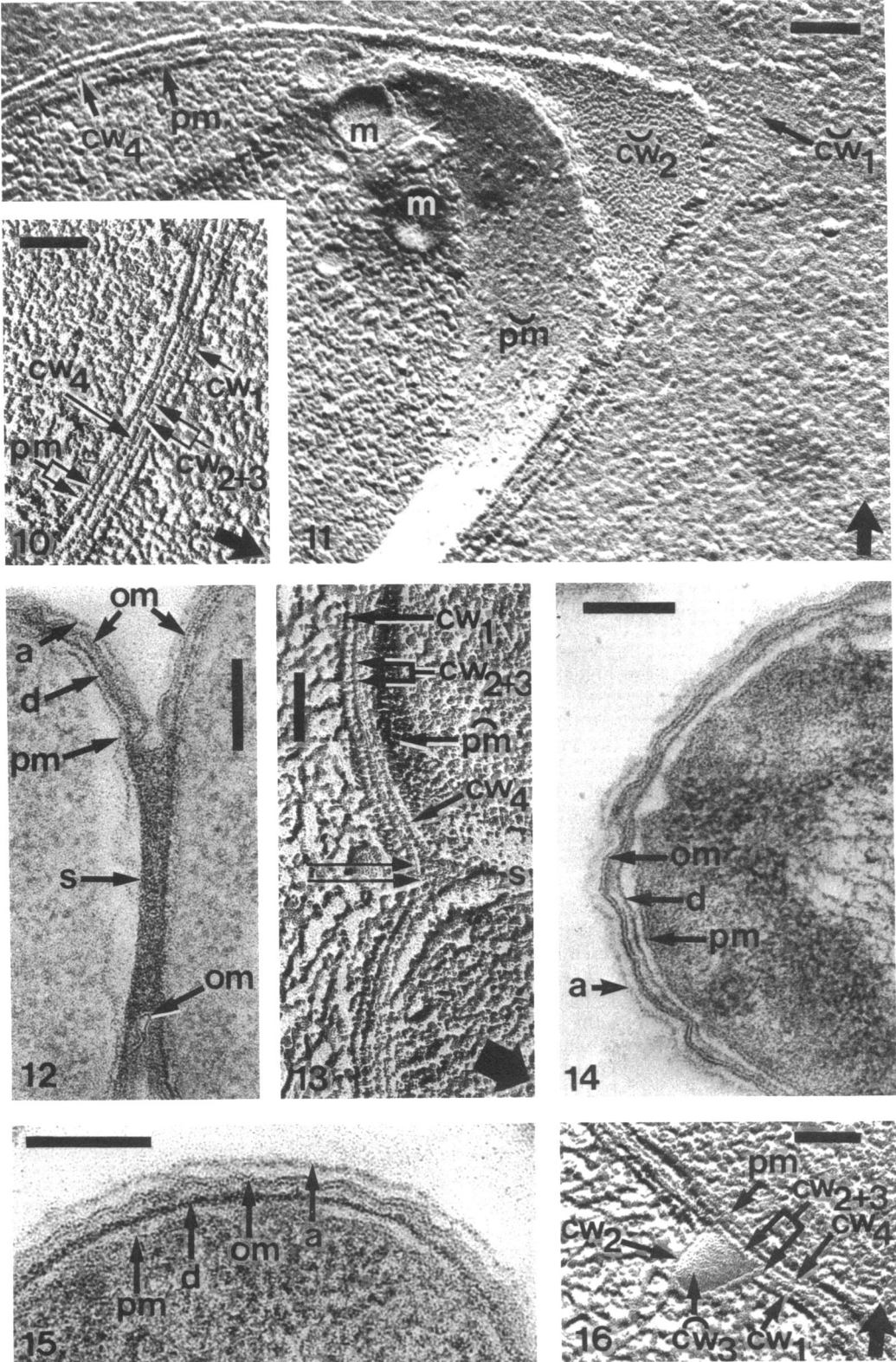


FIG. 10. Cell envelope seen in cross fracture in a preparation of heat-treated cells freeze-etched in the presence of glycerol (see Fig. 1B). Four main ridges are visible, cw 1, cw (2 + 3), cw 4, and pm, and both cw (2 + 3) and the plasma membrane (pm) appear as double ridges (double arrows). Figure 14 shows a cell from the same preparation in thin section.



fracture face of  $\check{c}w$  3 (Fig. 20) are located within the structure shown in section as om- and a-layer.

Figure 21 shows a concave portion of a cell envelope in the same preparation; here the pattern of closely packed granules characteristic of the fracture face  $\check{c}w$  2 is separated by a ridge from a smooth etched surface ( $\check{c}w$  3), which lies next to an ice surface. As in Fig. 20, the ice-filled region must correspond to the space between the outer membrane and the plasma membrane, and therefore the fracture face  $\check{c}w$  2 lies within the structure seen as om + a in section. The etched face  $\check{c}w$  3 is the inner surface of the outer membrane, as it appears after detachment from the inner part of the cell envelope by lysozyme treatment.

A similar relationship between the granular fracture face  $\check{c}w$  2 and a smooth etched surface  $\check{c}w$  3 is seen in Fig. 23, which represents a concave fragment from a preparation of cell walls treated with lysozyme by method E; the layers visible in thin section in this preparation (Fig. 30) were the outer membrane and additional layer only.

Some changes were observed in the structure of the plasma membranes after treatment of the cells with lysozyme by method B in the presence of sucrose and glycerol. As already mentioned, normal cells freeze-etched in the presence of glycerol showed internal fracture faces of the plasma membrane with the usual appearance of densely clustered particles on the  $\check{p}m$  and more scattered particles on the  $\check{p}m$ ; on both of these surfaces, irregularly shaped areas without particles were also visible. Similar areas without particles, usually having a round outline, were very common on both convex and concave fracture faces of the plasma membrane of spheroplasts prepared by method B (Fig. 24, 25, 27). The particle-free regions often protruded

beyond the smooth outline of the rest of the fracture face (Fig. 24, 27), possibly indicating that the structure of this portion of the membrane is mechanically weaker.

The concave fracture faces of plasma membranes of cells after lysozyme treatment also differed from those in untreated cells in the presence of small clusters of particles (Fig. 18, 26, 28). In Fig. 26, a ring-shaped group of particles is situated in a shallow depression in the concave fracture face,  $\check{p}m$ .

## DISCUSSION

The cell wall of *Acinetobacter* MJT/F5/5 shows in section (Fig. 1A) the structure typical of gram-negative bacteria with an additional outer layer, and the results of freeze-etching with and without glycerol also resemble those found for many other gram-negative organisms (e.g., 5, 10, 15, 16, 22). In the absence of glycerol, fracture within the cell envelope occurs only in the plasma membrane, which must therefore represent the weakest plane within the structure, and no indication is seen of ridges within cross-fractured cell walls. After glycerol treatment, the cross-fractured cell envelope appears thicker and consistently shows the arrangement of ridges shown in Fig. 1B. The grooves between these ridges must therefore contain some etchable material after glycerol treatment. The interpretation of these cross-fractured ridges in terms of the layers seen in thin section is indicated in Fig. 1A and 1B; this interpretation is based on comparisons of normal cell envelopes by the two techniques, and the layers are shown even more clearly by both techniques in the envelopes of heat-treated cells (Fig. 10, 14). The identification of the outer membrane as layer cw (2 + 3) in freeze-etched preparations also corresponds to the arrangement of layers seen at the point of septum

FIG. 11. Concave view of an oblique fracture through the envelope of a cell treated with lysozyme by method C and freeze-etched in the presence of glycerol. The concave fracture faces  $\check{p}m$ ,  $\check{c}w$  2, and  $\check{c}w$  1 are visible, and a hexagonal pattern is seen on  $\check{c}w$  1; m, mesosome.

FIG. 12. Thin section showing the region of septum formation in a dividing cell. The septum (s) has completely separated the daughter cells and is continuous with the dense layer (d) of the cell wall. The outer membrane (om) covers the zone of constriction but does not penetrate the septum.

FIG. 13. Cell envelope cross fractured at the region of ingrowth of a septum in a preparation freeze-etched in the presence of glycerol. The ingrowing septum (s) is continuous with cw 4, whereas cw (2 + 3) and cw 1 show a slight constriction only. The double nature of cw (2 + 3) is visible (double arrows).

FIG. 14. Thin section of a cell in a heat-treated preparation which may be compared with a normal cell (Fig. 15). The outer membrane (om), dense layer (d), and plasma membrane (pm) are seen more distinctly separated here, and in addition, the spacing between the plasma membrane and dense layer is greater; a, additional layer.

FIG. 15. Thin section of a normal cell, showing the plasma membrane (pm), dense layer (d), outer membrane (om), and additional layer (a).

FIG. 16. Cell envelope, cross fractured near to a surface bleb, in a preparation of normal cells freeze-etched in the presence of glycerol. The bleb is seen as a convex fracture face surrounded by a ridge, and at the base of the bleb both the ridge and the fracture face seem continuous with the double ridge of cw (2 + 3). The convex face is therefore part of  $\check{c}w$  3, but lacks the usual fibrillar appearance (compare with  $\check{c}w$  2 in the bleb shown in Fig. 9).

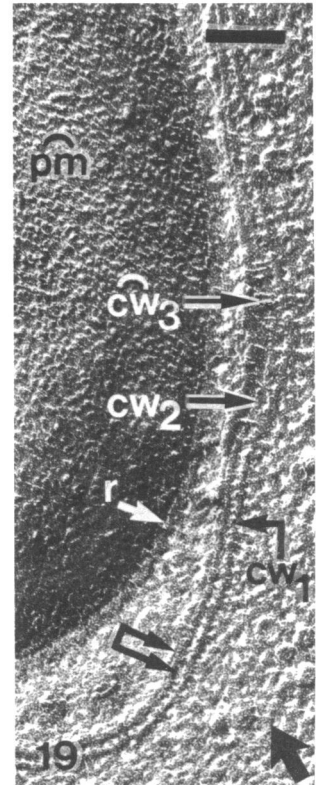
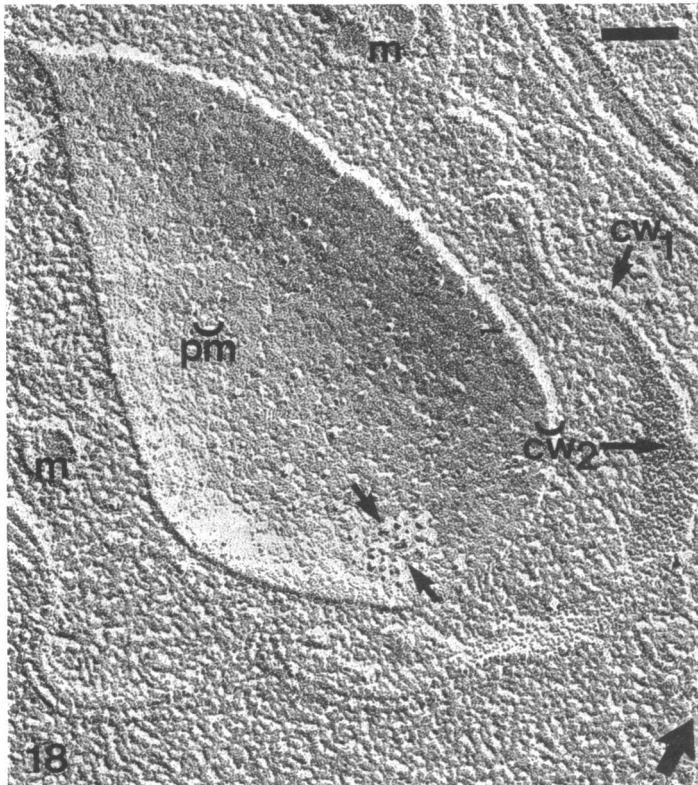
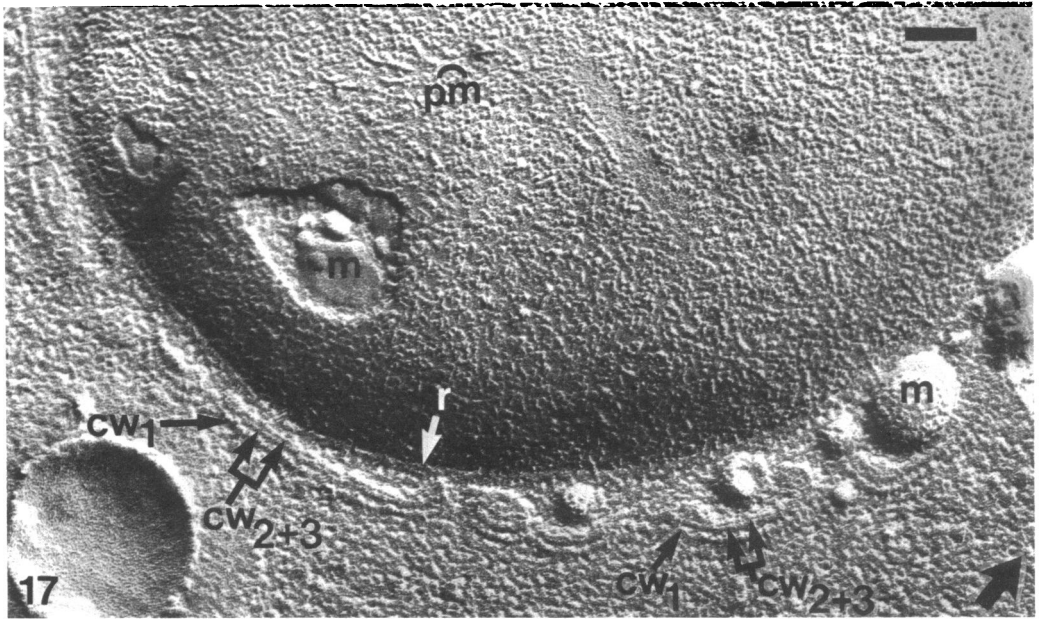
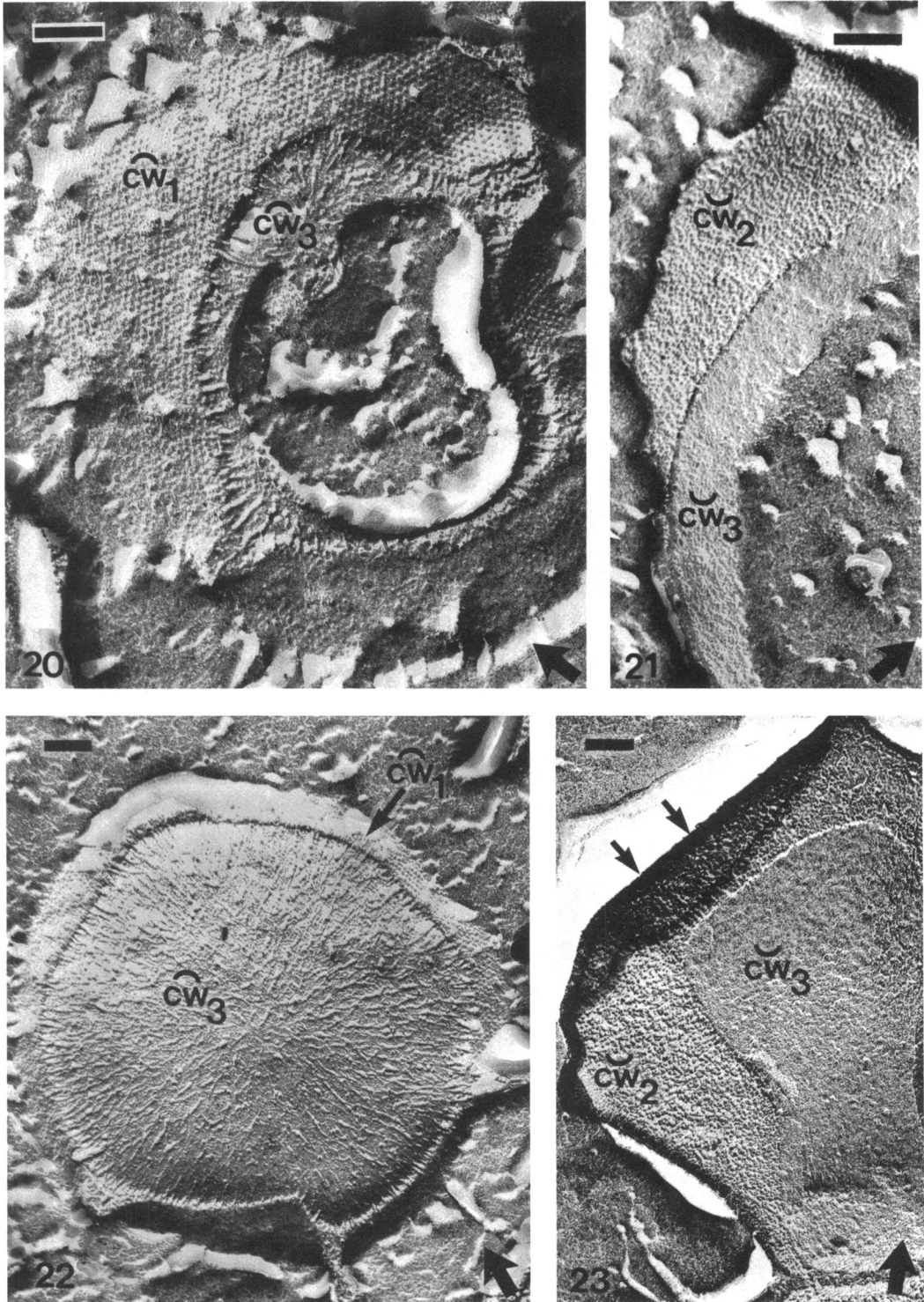


FIG. 17-19. A preparation of cells treated with lysozyme by method A and freeze-etched in the presence of glycerol.

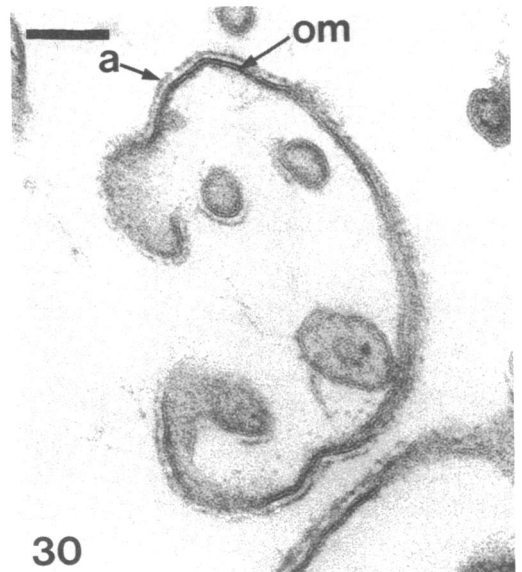
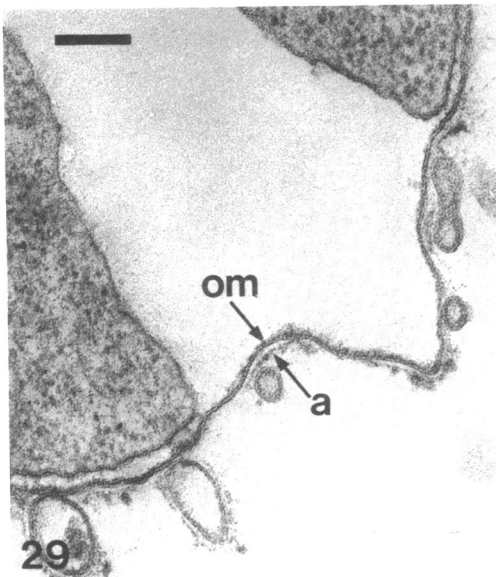
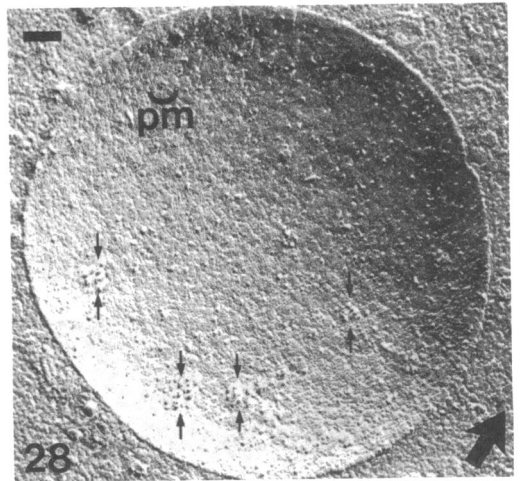
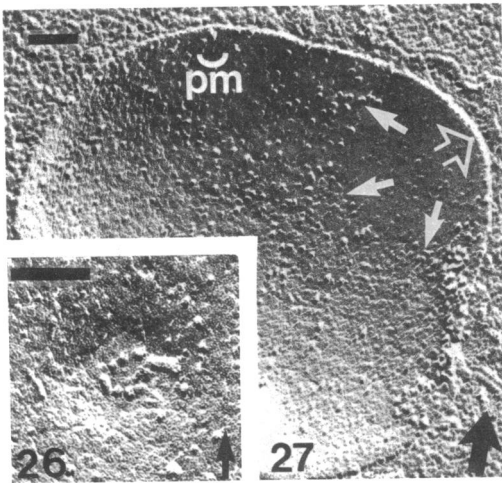
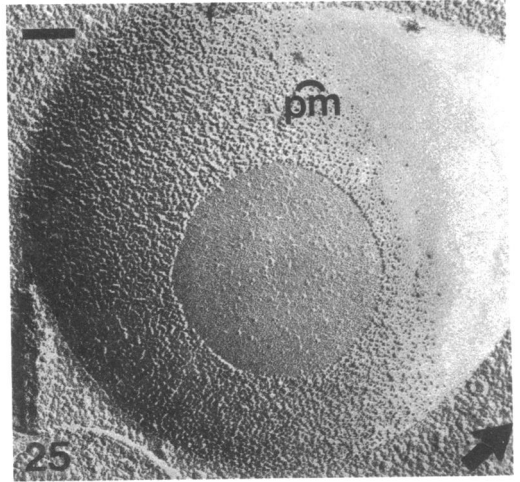
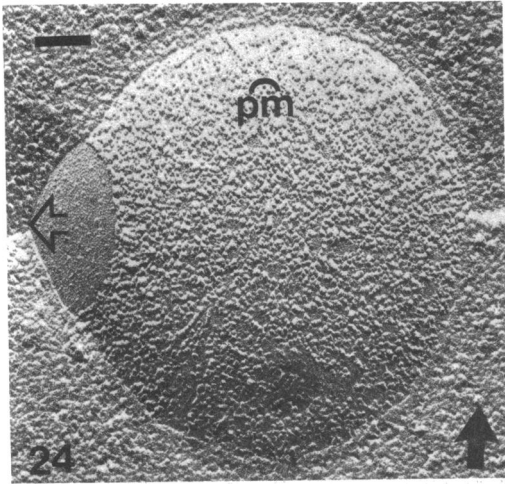
FIG. 17. The outer layers of the envelope, cw 1 and cw (2 + 3), are detached from the plasma membrane, of which the internal fracture face (pm) and the edge of the outer portion (r) are visible; cw 4 is not visible; m, mesosome.

FIG. 18. An oblique fracture seen in concave view shows the edge of cw 1 and the fracture face cw 2 with its characteristic granular surface, separated by ice from the concave fracture face (pm). In addition to the scattered particles usually seen on the pm, a cluster of particles is present (arrows).

FIG. 19. Region of cross fracture of the outer layers of the cell envelope, cw 1 and cw (2 + 3), is continuous with a region of more oblique fracture. The double ridge representing the cross-fractured layer cw (2 + 3) (double arrows) separates to reveal the internal fracture face cw 3. These outer layers are separated by a region of ice from the edge (r) of the outer portion of the plasma membrane and the internal fracture face (pm).



FIGS. 20-23—legends page 705



FIGS. 24-30—legends page 705

formation, whereas in Fig. 12 the outer membrane does not form part of the ingrowing septum, and in Fig. 13 the corresponding position is occupied by the double ridge of cw (2 + 3).

The main fracture faces within the cell wall,  $\hat{c}w$  2 and  $\hat{c}w$  3, are exposed after glycerol treatment almost as frequently as the internal fracture faces of the plasma membrane, and, therefore, a second plane of weakness in the envelope appears to be induced by the glycerol treatment.

The surface of the concave fracture face  $\hat{c}w$  2, consisting of closely packed particles smaller than those present on the plasma membrane, resembles that seen in nearly all the gram-negative bacteria so far studied by freeze-etching (5, 9, 10, 14-16, 21), whereas the convex face  $\hat{c}w$  3, with its fibrils and depressions, is similar to those seen in *Pseudomonas aeruginosa* (5) and *Acinetobacter* MJT/F5/199A (15). Because of the great similarity in architecture of the walls of gram-negative bacteria as seen in thin section, and because of the very similar appearance of the fracture faces revealed in different gram-negative bacteria, it seems likely that the zone of fracture within the wall is usually located in the same position in different bacteria. However, the relation of this position to the struc-

ture seen in section has proved difficult to establish conclusively (10). Several workers (5, 22) have suggested that the outer membrane fractures internally in the same way as the plasma membrane, but no evidence has been available to prove this. Forge et al. (4) showed that a cleavage plane was associated with vesicles consisting of the isolated outer membrane of a marine pseudomonad, but this did not provide evidence that the cleavage was internal, and the characteristic surface patterns of the fracture faces seen within the cell walls of most gram-negative bacteria were not revealed.

The present study of *Acinetobacter*, MJT/F5/5 has shown that when the outer membrane together with its surface subunits is detached from the underlying layers of the envelope by lysozyme treatment, as shown in thin section, both concave and convex fracture faces with their characteristic surface structures are revealed within the detached portion, om + a, and the appearance of Fig. 19 indicates that  $\hat{c}w$  3 results from an internal fracture of the outer membrane. In preparations containing the detached om + a layers without glycerol, both fracture faces  $\hat{c}w$  2 and  $\hat{c}w$  3 are seen, and, in addition, etching reveals the outer convex surface with its hexagonally arranged subunits and a smooth inner surface, assumed to be that

FIG. 20-23. Preparations of cell envelopes treated with lysozyme by methods D or E and freeze-etched in the absence of glycerol.

FIG. 20. Convex view of a cell envelope prepared by treatment with lysozyme (method D) shows the etched outer surface  $\hat{c}w$  1, the fibrillar fracture face  $\hat{c}w$  3, and an underlying space produced by the etching of an ice-filled region. Compare with a thin section of the same preparation (Fig. 29).

FIG. 21. Concave view of a cell envelope, prepared as in Fig. 20, shows the granular fracture face,  $\hat{c}w$  2, separated by a small ridge from a small ridge from a smooth etched face,  $\hat{c}w$  3. An etched ice surface is enclosed within  $\hat{c}w$  3.

FIG. 22. Convex view of a cell envelope prepared as in Fig. 20, with a small part of the outer surface  $\hat{c}w$  1 exposed by etching. A large area of the fracture face  $\hat{c}w$  3 shows a radial arrangement of fibrils similar to that seen in untreated cells freeze-etched in the presence of glycerol (Fig. 6).

FIG. 23. Concave view of a fragment of the cell envelope treated with lysozyme by method E, which shows the granular fracture face  $\hat{c}w$  2 and the smooth etched face  $\hat{c}w$  3 separated by a small ridge. The outer edge of this fragment has become detached from the surrounding ice and folded (arrows) during etching and replication. Fig. 30 shows the appearance of the same preparation in thin section.

FIG. 24-28. Spheroplasts prepared by lysozyme treatment (method B) and freeze-etched in the presence of glycerol show large areas of internal fracture of the plasma membrane.

FIG. 24. Particle-free area on the convex face  $\hat{p}m$  protrudes beyond the outline of the rest of the spheroplast.

FIG. 25. Circular particle-free zone on the  $\hat{p}m$ .

FIG. 26. Ring-shaped cluster of particles in a shallow depression of the  $\hat{p}m$ .

FIG. 27. Particle-free zone on the concave face  $\hat{p}m$  protrudes beyond the outline of the rest of the fracture face.

FIG. 28. The concave fracture face  $\hat{p}m$ , in a spheroplast, shows small clusters of particles (arrows), as well as the scattered particles normally present on this face.

FIG. 29. Thin section of a preparation of cells treated with lysozyme by method D. The dense layer of the cell wall is no longer visible, and the remaining layers, the outer membrane (om) and additional layer (a), are separated from the plasma membrane by a space. At one part of the surface, the protoplast has retracted some distance from the outer membrane.

FIG. 30. Thin section of a preparation of cell envelope fragments treated with lysozyme (method E). The outer membrane (om) and additional layer (a) are present; the dense layer is not visible.

of  $\check{c}w$  3. This is regarded as convincing evidence that an internal fracture of the outer membrane gives rise to the characteristic fracture faces  $\check{c}w$  2 and  $\check{c}w$  3.

The fracture plane in these detached outer membranes cannot lie between the outer membrane itself and the surface subunits, because fracture at this level, which occurs very rarely in glycerol-treated intact cells, gives a smooth convex surface  $\check{c}w$  2 (Fig. 7) and a smooth or hexagonally patterned concave surface  $\check{c}w$  1 (Fig. 8, 9, 11). Also, we have shown that similar results to those reported here are obtained with a preparation of *Pseudomonas fluorescens* (unpublished data), whose detached outer membranes do not carry an outer layer of surface subunits.

It seems surprising that the outer membranes, when detached, will fracture internally in the absence of glycerol, whereas the same fracture faces in the intact cell envelope only result from fracture with glycerol present. We assume that the most probable explanation is that in the intact envelope without glycerol the plasma membrane is close to the outer membrane and forms a weaker zone which fractures preferentially, whereas in the lysozyme-treated envelope the outer membrane together with the subunits is surrounded by ice, at a greater distance from the plasma membrane, and the relative resistance to fracture is changed.

The fracture of detached outer membranes was not observed in our earlier study of *Acinetobacter* MJT/F5/199A (15), in which spheroplasts were prepared by a method very similar to method A of the present paper and were freeze-etched in the presence of glycerol. The fact that this study did not yield results similar to those produced by method A in MJT/F5/5 (Fig. 17-19) seems more likely to be due to a difference between the organisms than to any difference in methods.

The lack of complementarity between the internal fracture faces of the outer membrane ( $\check{c}w$  2 and  $\check{c}w$  3) is very marked, as there seems to be no relation in structure between the closely packed particles of  $\check{c}w$  2 and the fibrillar surface of  $\check{c}w$  3. It seems probable that the fibrils of  $\check{c}w$  3 arise by plastic deformation during fracture of some component within the outer membrane. The radial arrangement of the fibrils (Fig. 6, 22) would support this idea, and the occurrence of plastic deformation during freeze-fracture has been established (1-3). Although some lack of complementarity is observed in many other kinds of membrane, the extent of dissimilarity seen here is unusual; it is

perhaps correlated with the characteristic chemical composition and selective permeability properties of the outer membranes of gram-negative bacteria. The process of fracture in the outer membranes also differs from that of the plasma membranes in being very limited in extent in preparations freeze-etched in the absence of glycerol and in being completely prevented by previous glutaraldehyde fixation. Both these properties also are presumably influenced by the chemical composition of the different types of membrane.

The significance of the clusters of particles seen in the present study of *Acinetobacter* MJT/F5/5 on the concave fracture face of the plasma membrane in lysozyme-treated preparations (Fig. 18, 26, 28) is not known, but it is suggested that they might represent sites at which mesosomes have been extruded. The size of the clusters is similar to the size of extruded mesosomes, and the process of extrusion is evidently taking place in the preparation shown in Fig. 17-19, after the shorter period of lysozyme treatment, because some mesosomes are just within the cytoplasm whereas others are outside the plasma membrane. None were seen passing through the plasma membrane, although this process has been observed previously in protoplasts of *Bacillus stearothermophilus* (13). The small clusters and ring-shaped groups (Fig. 26) of particles are very similar in appearance to those seen at the point of discharge of mucocysts in *Tetrahymena* (11, 12), which suggests that they may be connected with a phenomenon of membrane fusion or extrusion of vesicles.

#### ACKNOWLEDGMENTS

We acknowledge the support of the European Molecular Biology Organization (to U. B. S.), the Science Research Council (to M. J. T.), and the Sir Halley Stewart Trust (to A. M. G.). We thank the Wellcome Trust for the loan of the AEI-EM6B electron microscope and the Medical Research Council Laboratory of Molecular Biology for the use of the Balzer freeze-etching apparatus.

We are very grateful to R. A. Parker for skilled technical assistance.

#### LITERATURE CITED

1. Bullivant, S. 1973. Freeze-etching and freeze-fracturing, p. 67-112. In J. K. Koehler (ed.), *Advanced techniques in biological electron microscopy*. Springer-Verlag, Berlin.
2. Bullivant, S., D. G. Rayns, W. S. Bertaud, J. P. Chalcraft, and G. F. Grayston. 1972. Freeze-fractured myosin filaments. *J. Cell Biol.* **55**:520-524.
3. Clark, A. W., and D. Branton. 1968. Fracture faces in frozen outer segments from the guinea pig retina. *Z. Zellforsch. Mikrosk. Anat.* **91**:586-603.
4. Forge, A., J. W. Costerton, and K. A. Kerr. 1973. Freeze-etching and X-ray diffraction of the isolated double-track layer from the cell wall of a gram-negative

- marine pseudomonad. *J. Bacteriol.* **113**:445-451.
5. Gilleland, H. E., J. D. Stinnet, I. L. Roth, and R. G. Eagon. 1973. Freeze-etch study of *Pseudomonas aeruginosa*: localization within the cell wall of an ethylenediaminetetraacetate-extractable component. *J. Bacteriol.* **113**:417-432.
  6. Glauert, A. M., and M. J. Thornley. 1971. Fine structure and radiation resistance in *Acinetobacter*: a comparison of a range of strains. *J. Cell Sci.* **8**:19-41.
  7. Juni, E. 1972. Interspecies transformation of *Acinetobacter*: genetic evidence for a ubiquitous genus. *J. Bacteriol.* **112**:917-931.
  8. Moor, H., and K. Mühlethaler. 1963. Fine structure in frozen-etched yeast cells. *J. Cell Biol.* **17**:609-628.
  9. Remsen, C. C., and D. G. Lundgren. 1966. Electron microscopy of the cell envelope of *Ferrobacillus ferrooxidans* prepared by freeze-etching and chemical fixation techniques. *J. Bacteriol.* **92**:1765-1771.
  10. Remsen, C. C., and S. W. Watson. 1972. Freeze-etching of bacteria. *Int. Rev. Cytol.* **33**:253-296.
  11. Satir, B., C. Schooley, and P. Satir. 1973. Membrane fusion in a model system. *J. Cell Biol.* **56**:153-176.
  12. Satir, B., C. Schooley, and P. Satir. 1973. Membrane reorganization during secretion in *Tetrahymena*. *Nature (London)* **235**:53-54.
  13. Sleytr, U. B. 1970. Fracture faces in intact cells and protoplasts of *Bacillus stearothermophilus*. A study by conventional freeze-etching and freeze-etching of corresponding fracture moieties. *Protoplasma* **71**:295-312.
  14. Sleytr, U. B., and M. Kocur. 1973. Structure of *Micrococcus denitrificans* and *Micrococcus halodenitrificans* revealed by freeze-etching. *J. Appl. Bacteriol.* **36**:19-22.
  15. Sleytr, U. B., and M. J. Thornley. 1973. Freeze-etching of the cell envelope of an *Acinetobacter* species which carries a regular array of surface subunits. *J. Bacteriol.* **116**:1383-1397.
  16. Swanson, J. 1972. Studies on gonococcus infection. II. Freeze-fracture, frozen-etch studies on gonococci. *J. Exp. Med.* **136**:1258-1271.
  17. Thorne, K. J. I., M. J. Thornley, and A. M. Glauert. 1973. Chemical analysis of the outer membrane and other layers of the cell envelope of *Acinetobacter* sp. *J. Bacteriol.* **116**:410-417.
  18. Thornley, M. J. 1967. A taxonomic study of *Acinetobacter* and related genera. *J. Gen. Microbiol.* **49**:211-257.
  19. Thornley, M. J., and A. M. Glauert. 1968. Fine structure and radiation resistance in *Acinetobacter*: studies on a resistant strain. *J. Cell Sci.* **3**:273-294.
  20. Thornley, M. J., A. M. Glauert, and U. B. Sleytr. 1973. The isolation of outer membranes with an ordered array of surface subunits from *Acinetobacter*. *J. Bacteriol.* **114**:1294-1308.
  21. Van Gool, A. P. 1972. Ultrastructure of *Nitrosomonas europaea* cells as revealed by freeze-etching. *Arch. Mikrobiol.* **82**:120-127.
  22. Van Gool, A. P., and N. Nanninga. 1971. Fracture faces in the cell envelope of *Escherichia coli*. *J. Bacteriol.* **108**:474-481.